Triclinic phase in tilted (001) oriented BiFeO 3 epitaxial thin films

Li Yan, Hu Cao, Jiefang Li, and D. Viehland

Citation: Applied Physics Letters **94**, 132901 (2009); doi: 10.1063/1.3110972
View online: http://dx.doi.org/10.1063/1.3110972
View Table of Contents: http://scitation.aip.org/content/aip/journal/apl/94/13?ver=pdfcov
Published by the AIP Publishing

Triclinic phase in tilted (001) oriented $BiFeO_3$ epitaxial thin films

Li Yan,[a] Hu Cao, Jiefang Li, and D. Viehland
Department of Materials Science and Engineering, Virginia Tech, Blacksburg, Virginia 24061, USA

(Received 13 January 2009; accepted 11 March 2009; published online 30 March 2009)

We report a triclinic phase in perovskite $BiFeO_3$ (BFO) epitaxial thin films grown on (130) and (120) oriented $SrTiO_3$ substrates. The lattice constants of the BFO thin films changed with tilt of the substrates from (001) toward (110). These lattice parameters result from the epitaxially engineering of structurally bridging phases of the lowest possible symmetry. © *2009 American Institute of Physics*. [DOI: 10.1063/1.3110972]

The perovskite $BiFeO_3$ (BFO) is a multiferroic material which has both ferroelectric and ferromagnetic orders.[1–3] Its Curie temperature is 830 °C and its Néel temperature is 370 °C.[4–8] At room temperature, bulk BFO single crystals have a distorted rhombohedral (R) structure with lattice parameters of $(a_r, \alpha_r)=(3.96\ \text{Å}, 89.4°)$. Along [111], BFO has a threefold axis, where the Bi^{3+} and Fe^{3+} cations are displaced from their symmetric positions.[1,9–12] This asymmetry generates a spontaneous polarization along the [111]. In addition, there is an alignment of spins the along [111], whose moments are slightly canted from this direction resulting in a weak ferromagnetic moment.

Epitaxial BFO thin layers have also been reported.[13] The symmetry of the BFO layers has been shown to be notably distorted from that of the R phase in bulk crystals.[14] Investigations by high resolution x-ray diffraction (XRD)[15,16] have shown that films grown on (001), (110), and (111) $SrTiO_3$ (STO) substrates, respectively, have a monoclinic *A* (M_A) structure with lattice parameters of $(a_M/\sqrt{2}, b_M/\sqrt{2}, c_M, \beta)=(3.973\ \text{Å}, 3.907\ \text{Å}, 3.997\ \text{Å}, 89.2°)$, where the polarization is constrained to the (001) plane; monoclinic *B* with lattice parameter of $(a_M/\sqrt{2}, c_M, \beta)=(3.985\ \text{Å}, 3.888\ \text{Å}, 89.35°)$, where *P* is constrained to the (110) plane and rhombohedral (R) with lattice parameters equivalent to that of bulk crystals, where the polarization is constrained to the (111) direction.

Monoclinic domain engineered phases have previously been reported in perovskite $(1-x)Pb(Mg_{1/3}Nb_{2/3})O_3$-$xPbTiO_3$ (PMN-PT) and $(1-x)Pb(Zn_{1/3}Nb_{2/3})$-$xPbTiO_3$ (PZN-PT) single crystals.[17–27] Domain engineering was achieved by cooling under electric fields applied to high symmetry [i.e., (001), (110), or (111)] directions, or orientations different than that of the spontaneous polarization P_s in the zero-field-cooled state.[26,27] Low symmetry structurally bridging monoclinic phases have been shown to be important in enhancing properties in the vicinity of a morphtropic phase boundary.

Analogously, in perovskite thin layers, low symmetry structurally bridging phases can be epitaxially engineered by lattice parameter mismatch and substrate orientation.[14] Theoretical investigations have shown that epitaxy can be used as a thermodynamic variable by which to control phase stability in perovskites. Lattice parameters of films can be altered in perovskites in order to relax epitaxial stress.[28] Although the magnitude of the constraint stress can be change by various method (such as substrates, buffer layers, or film thickness), a more important factor in the engineering of phase stability is the direction along which this constraint stress is applied. Prior investigations have been limited to the study of higher symmetry (001), (110), and (111) oriented substrates. The influences of lower symmetry oriented substrates have not yet been investigated on the phase stability of perovskite layers.

Here, we have investigated a method of epitaxial engineering of the phase stability of low symmetry perovskite by altering the direction of the constraint stress, via selecting low symmetry (or interim) orientations of single crystal substrates. For example, by using (130) or (120) oriented STO substrates, the constraint stress can be controlled to lie between the (100) and (110) directions. By this method, we have found it possible to control the crystal structure and lattice parameters in epitaxial films. We have observed a triclinic phase in BFO when deposited on tilted (001) STO substrates, where the lattice parameter of the films can be varied from 3.90 to 4.08 Å.

Epitaxial layers of BFO were grown by pulsed laser deposition on (100), (130), (120), (110), and (111) $SrTiO_3$ substrates that had been ultrasonically cleaned. The layers were kept to a thickness of ~40 nm to prevent relaxation of the constraint stress. Films were deposited using a KrF laser (wavelength of 248 nm) by a Lambda 305i: using energy densities of 1.2 J/cm^2. The distance between the substrate and target was 6 cm and the base vacuum of the chamber was $<10^{-5}$ Torr. During film deposition, the oxygen pressure was 100 mTorr. The crystal structure of the films was measured using a Philips X'pert high resolution x-ray diffractometer equipped with a two bounce hybrid monochromator and an open three-circle Eulerian cradle. The analyzer was a Ge (220) cut crystal which had a θ-resolution of 0.0068°.

The lattice constants of the variously oriented $BiFeO_3$ in single unit cell representations are summarized in Table I. The (111) oriented BFO thin films were rhombohedral (*R*) with lattice constant of $a_r=3.959$ Å and $\alpha_r=89.48°$, which is the same as bulk materials as previously reported.[9–12] For (001) and (110) BFO, $a_m=b_m\neq c_m$, and $\alpha=\gamma=90°\neq\beta$. In this case, the diagonals in the a and b plane are normal to each other in the unit cell. For (110) BFO, $c<a$, whereas for (001) $c>a$. As a consequence, the stable structures are M_B and M_A, respectively, with lattice constant of $(a_M/\sqrt{2}=3.996(7)\ \text{Å}, b_M/\sqrt{2}=3.952(8)\ \text{Å}, c_M$

[a]Electronic mail: lyan@vt.edu. Tel.: 540-231-6928.

TABLE I. Lattice constant of $BiFeO_3$ thin films in single unit cell.

	Phase	Angle from (100) (deg)	a (Å)	b (Å)	c (Å)	α (°)	β (°)	γ (°)
(110)	M_B in double unit cell	Tilted 45	3.974(8)	3.974(8)	3.925(3)	89.46	89.46	89.37
(120)	Triclinic	Tilted 26	3.955(5)	4.011(4)	3.912(5)	89.52	89.51	89.34
(130)	Triclinic	Tilted 18	3.926(5)	4.041(9)	3.909(3)	89.52	89.51	89.30
(100)	M_A in double unit cell	Tilted 0	3.903(4)	3.903(4)	4.075(6)	89.53	89.53	89.53
(111)	Rhombohedral	...	3.959(2)	3.959(2)	3.959(2)	89.48	89.48	89.48

$=3.925(3)$ Å, $\beta=89.24°$) and ($a_M/\sqrt{2}=3.919(5)$ Å, $b_M/\sqrt{2}=3.887(2)$ Å, $c_M=4.075(6)$ Å, $\beta=89.34°$) in a double unit cell representation.

However, a triclinic phase was found for (130) and (120) oriented BFO thin films, which were 26° and 18° titled from the (100). Because BFO is not tetragonal (T), orthorhombic (O), or rhombohedral (R), we must use a parallelogram model to perform calculations to determine the lattice constants and crystal structure. First, we calculated the gray plane in Fig. 1(a), which is normal to the substrate, as circled by the blue dashed plane in the figure. From the distances b'', m', and n' that we measured directly, we can calculate a', b', t, and all angles in this plane [see Fig. 1(b)]. Next, we calculated the gray plane in Figs. 1(c) and 1(d). From p and q that were directly measured and n which was calculated above, we can determine c and r. Accordingly, all the lattice constants and angles have been so determined. All the original XRD peaks used in the calculation are shown in Figs. 1(e) and 1(f). We then used these lattice constants to build a model, from which we can predict the lattice constants independently of the first step above. By comparing all the predicted values to those that were directly measured, we found a convergence of values. For example, the predicted values of the interplanar spacings $d_{(111)}$ and $d_{(010)}$ were 6.832(4) and 3.955(1) Å for the (120) films, whereas the measured values were 6.831(5) and 3.954(3) Å: a difference of only 0.01% and 0.02% for $d_{(111)}$ and $d_{(010)}$ between prediction and measurement. The triclinic lattice parameters of (120) and (130) BFO films are $(a_t, b_t, c_t; \alpha_t, \beta_t, \gamma_t)$=[3.955(5) Å, 4.011(4) Å, 3.912(5) Å, 89.52°, 89.51°, 89.34°] and $(a_t, b_t, c_t; \alpha_t, \beta_t, \gamma_t)$ =[3.926(5) Å, 4.041(9) Å, 3.909(3) Å, 89.52°, 89.51°, 89.30°], respectively. The (130) and (120) BFO films can only be described as by a single cell triclinic structure, which cannot fit to any higher symmetry multicell structural representation.

The (100), (130), (120), and (110) oriented BFO films were deposited on STO single crystal substrates, which were 0°, 18°, 26°, and 45° titled from the (100) plane. Figure 2 shows the lattice parameters of these various oriented BFO layers as a function of the tilt angle from the (100) toward the (110). The blue dashed line represents the lattice constant of the STO substrate, which was $a_c=3.90$ Å. The lattice parameters from left to right are for (100), (130), (120), and (110) oriented BFO films. The angles between the lattice and substrate are marked in bold on top of the points. As the angle between the lattice and substrate was increased from 0° (in plane) to 45° (out of plane), the lattice parameters of BFO increased gradually from 3.90 to 3.97 Å; whereas the c lattice parameter decreased from 4.08 to 3.97 Å. The relationship between the tilt and the BFO lattice parameters are nearly linear, indicating that elastic constraint is an important factor. With increasing tilt, the in-plane lattice parameters gradually increased as the compressive stress was increased, whereas the out-of-plane parameter gradually decreased.

In addition, we found when the substrate was changed from (100) to (110) that the in-plane lattice constants were also slightly increased with respect to those out of plane from 3.90 to 3.92 Å. The cause for this is the anisotropic nature of the constraint stress along the in-plane directions. For (100) BFO films, the compressive stress from the substrate was isotropic. However, for (130), (120), and (110) BFO films, the in-plane compressive stress becomes increasingly anisotropic with increasing tilt angle away from the

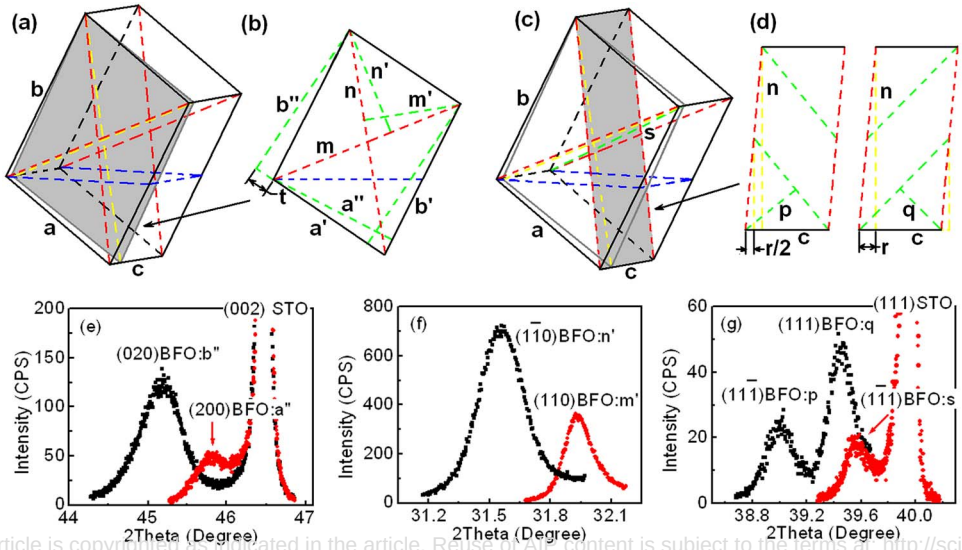

FIG. 1. (Color online) [(a)–(d)] Illustration of the planes in the unit cell which were used to calculate the triclinic lattice constants and tilt angles for $BiFeO_3$. [(e)–(f)] X-ray results of BFO peaks which are used in the calculation.

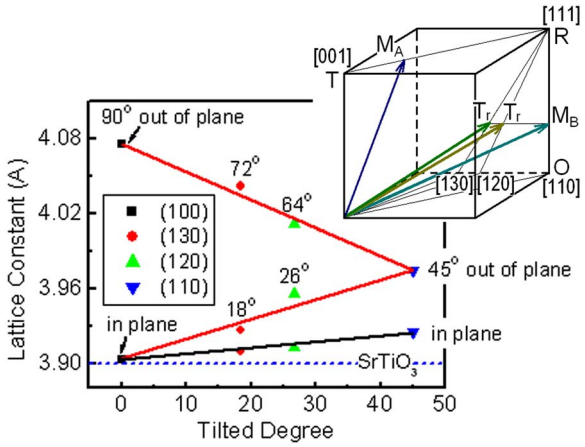

FIG. 2. (Color online) Lattice constants of (100), (130), (120), and (110) oriented $BiFeO_3$ thin films as a function of tilt angle, demonstrating the relationship between the lattice constants of $BiFeO_3$ and the angle between the film and substrate. Insert shows that M_A, triclinic, triclinic, and M_B are the results of the combination of the constraint stress from the (100), (130), (120), and (110) substrates and the stable R phase of BFO, respectively.

(001). In the case of (110), the compressive stress along the $\langle 001 \rangle$ is lower than that along $\langle 1\bar{1}0 \rangle$: this make the lattice parameter for (110) layers larger than that of (001).

The insert of Fig. 2 can be used to explain the formation of structurally bridging triclinic and monoclinic phases in BFO films. Bulk BFO has a rhombohedral structure which is distorted from cubic along the [111]. Epitaxial stress applied by the substrate along [100], [110], [120], and [130] tends to compress the epitaxial thin films to T, O, M_A and M_C structures, respectively. The combination of the constraint stress from the substrate and the stable R phase of BFO results in net symmetries of M_A, M_B, triclinic, and triclinic, respectively. Using the understanding of our approach, we can predict/design crystal structures for other oriented epitaxial films. For example, if a R phase is deposited on (110), (113), (112), (223), (111), and (221) oriented substrates, a stable M_B structure can be expected, where the lattice parameter c_m will increase gradually on going from (110), (113), (112), to (223) orientations. However, (111) films will remain R with $c=a=b$; and (221) layers will be M_A with $c_m > a_m = b_m$.

In summary, we report a method by which to epitaxial engineer low symmetry phases in ferroelectric perovskites: the selection of tilted (001) single crystal substrates. Using this approach, we have developed triclinic BFO layers grown on (130) and (120) STO substrates that structurally bridge M_A and M_B monoclinic phases, where the lattice parameters can be varied from 3.90 to 4.08 Å.

We acknowledge financial support from the U.S. Department of Energy under Contract No. DE.-AC02-98CH10886, Office of the Air-Force Office of Scientific Research under Contract No. FA 9550-06-1-0410, and the Office of Naval Research under Grant N00014-06-1-0204.

[1] S. V. Kiselev, R. P. Ozerov, and G. S. Zhdanov, Sov. Phys. Dokl. **7**, 742 (1963).
[2] G. A. Smolenskii and I. Chupis, Sov. Phys. Usp. **25**, 475 (1982).
[3] E. K. H. Salje, *Phase Transitions in Ferroelastic and Co-elastic Crystals* (Cambridge University Press, Cambridge, 1990).
[4] Yu. E. Roginskaya, Yu. Ya. Tomashpol'skii, Yu. N. Venevtsev, V. M. Petrov, and G. Zhdanov, Sov. Phys. JETP **23**, 47 (1966).
[5] Yu. N. Venevtsev, G. Zhdanov, and S. Solov'ev, Sov. Phys. Crystallogr. **4**, 538 (1960).
[6] G. A. Smolenskii, V. Isupov, A. Agranovskaya, and N. Krainik, Sov. Phys. Solid State **2**, 2651 (1961).
[7] P. Fischer, M. Polomskya, I. Sosnowska, and M. Szymanski, J. Phys. C **13**, 1931 (1980).
[8] G. A. Smolenskii, V. Yudin, E. Sher, and Yu. E. Stolypin, Sov. Phys. JETP **16**, 622 (1963).
[9] C. Michel, J.-M. Moreau, G. D. Achenbach, R. Gerson, and W. J. James, Solid State Commun. **7**, 701 (1969).
[10] J. D. Bucci, B. K. Robertson, and W. J. James, J. Appl. Crystallogr. **5**, 187 (1972).
[11] J. R. Teague, R. Gerson, and W. J. James, Solid State Commun. **8**, 1073 (1970).
[12] I. Sosnowska, T. Perterlin-Neumaier, and E. Steichele, J. Phys. C **15**, 4835 (1982).
[13] J. Wang, J. Neaton, H. Zheng, V. Nagarajan, S. Ogale, B. Liu, D. Viehland, V. Vaithyanathan, D. Schlom, U. Waghamare, N. A. Spadlin, K. M. Rabe, M. Wuttig, and R. Ramesh, Science **299**, 1719 (2003).
[14] J. Li, J. Wang, M. Wuttig, R. Ramesh, N. Wang, B. Ruette, A. P. Pyatakov, A. K. Zvezdin, and D. Viehland, Appl. Phys. Lett. **84**, 5261 (2004).
[15] G. Xu, H. Hiraka, G. Shirane, J. Li, J. Wang, and D. Viehland, Appl. Phys. Lett. **86**, 182905 (2005).
[16] G. Xu, J. Li, and D. Viehland, Appl. Phys. Lett. **89**, 222901 (2006).
[17] S.-E. Park and T. R. Shrout, J. Appl. Phys. **82**, 1804 (1997).
[18] S. F. Liu, S.-E. Park, T. R. Shrout, and L. E. Cross, J. Appl. Phys. **85**, 2810 (1999).
[19] B. Noheda, D. E. Cox, G. Shirane, S. E. Park, L. E. Cross, and Z. Zhong, Phys. Rev. Lett. **86**, 3891 (2001).
[20] D. La-Orauttapong, B. Noheda, Z. G. Ye, P. M. Gehring, J. Toulouse, D. E. Cox, and G. Shirane, Phys. Rev. B **65**, 144101 (2002).
[21] B. Noheda, Z. Zhong, D. E. Cox, G. Shirane, S. E. Park, and P. Rehrig, Phys. Rev. B **65**, 224101 (2002).
[22] K. Ohwada, K. Hirota, P. Rehrig, Y. Fujii, and G. Shirane, Phys. Rev. B **67**, 094111 (2003).
[23] J. M. Kiat, Y. Uesu, B. Dkhil, M. Matsuda, C. Malibert, and G. Calvarin, Phys. Rev. B **65**, 064106 (2002).
[24] Z. G. Ye, B. Noheda, M. Dong, D. Cox, and G. Shirane, Phys. Rev. B **64**, 184114 (2001).
[25] B. Noheda, D. E. Cox, G. Shirane, J. Gao, and Z. G. Ye, Phys. Rev. B **66**, 054104 (2002).
[26] H. Cao, F. Bai, N. Wang, J. Li, D. Viehland, G. Xu, and G. Shirane, Phys. Rev. B **72**, 064104 (2005).
[27] H. Cao, J. Li, D. Viehland, and G. Xu, Phys. Rev. B **73**, 184110 (2006).
[28] K. Saito, A. Ulyanenkov, V. Grossmann, H. Ress, L. Bruegemann, H. Ohta, T. Kurosawa, S. Ueki, and H. Funakubo, Jpn. J. Appl. Phys., Part 1 **45**, 7311 (2006).